Available online at www.sciencedirect.com
SCIENCE DIRECT
ELSEVIER
Mutation Research 557 (2004) 1–6
MR
Genetic Toxicology and Environmental Mutagenesis
www.elsevier.com/locate/gentox
Community address: www.elsevier.com/locate/mutres

Genotoxicity of microcystin-LR in human lymphoblastoid TK6 cells

Li Zhan [a,b], Hiroko Sakamoto [a], Mayumi Sakuraba [a], De-Sheng Wu [b], Li-Shi Zhang [b], Takayoshi Suzuki [a], Makoto Hayashi [a], Masamitsu Honma [a,*]

[a] *Division of Genetics and Mutagenesis, National Institute of Health Sciences, 1-18-1 Kamiyoga, Setagaya-ku, Tokyo 158-8501, Japan*
[b] *West China School of Public Health, Sichuan University, Chengdu 610041, China*

Received 6 June 2003; received in revised form 22 September 2003; accepted 22 September 2003

Abstract

Toxic cyanobacteria (blue-green algae) water blooms have become a serious problem in several industrialized areas of the world. Microcystin-LR (MCLR) is a cyclic heptapeptidic toxin produced by the cyanobacteria. In the present study, we used human lymphoblastoid cell line TK6 to investigate the in vitro genotoxicity of MCLR. In a standard 4 h treatment, MCLR did not induce a significant cytotoxic response at <80 μg/ml. In a prolonged 24 h treatment, in contrast, it induced cytotoxic as well as mutagenic responses concentration-dependently starting at 20 μg/ml. At the maximum concentration (80 μg/ml), the micronucleus frequency and the mutation frequency at the heterozygous thymidine kinase (*TK*) locus were approximately five-times the control values. Molecular analysis of the *TK* mutants revealed that MCLR specifically induced loss of heterozygosity at the *TK* locus, but not point mutations or other small structural changes. These results indicate that MCLR had a clastogenic effect. We discuss the mechanisms of MCLR genotoxicity and the possibility of its being a hepatocarcinogen.

Keywords: Cyanobacteria; Microcystin-LR; Micronucleus test; TK-gene mutation

1. Introduction

Water pollution by cyanobacteria (blue-green algae) causes serious environmental and public health problems in several areas of the world [1–3]. Some genera, such as *Microsystis*, *Oscillatoria*, and *Anabaena* produce microcystines, cyclic heptapeptides, with potent hepatotoxic activity. Fifty different cyanobacterial microcystines have been discovered. They have caused the death of fish, birds, wild animals, and livestock [1,4] and sometimes have had adverse health effects on humans through contaminated residential water supplies [5,6].

Microcystin-LR (MCLR) is the most toxic microcystine. Only 1–2 μg MCLR given intraperitoneally is lethal to mice, with most accumulating in the liver [7,8]. While MCLR hepatotoxicity has been well documented in vitro and in vivo [9–12], few reports describe its genotoxicity. MCLR is not genotoxic in the Ames test, although cyanobacterial extracts are, both with and without metabolic activation [13]. In a human cancer cell line, on the other hand, MCLR induces point mutations, and it produces DNA fragmentation and degradation in mouse liver in vivo [14,15].

* Corresponding author. Tel.: +81-3-3700-1141x434; fax: +81-3-3700-2348.
E-mail address: honma@nihs.go.jp (M. Honma).

1383-5718/$ – see front matter © 2003 Elsevier B.V. All rights reserved.
doi:10.1016/j.mrgentox.2003.09.006

To evaluate the in vitro genotoxicity of MCLR, we used the in vitro micronucleus (MN) assay and the thymidine kinase (*TK*) gene mutation assay on treated human lymphoblatoid TK6 cells [16,17]. The *TK* gene mutation assay is capable of detecting a wide range of genetic damage, including gene mutations, large scale chromosomal changes, recombination, and aneuploidy. Most of the changes occur in human tumors and are presumably relevant to carcinogenesis. Use of a human cell line makes this genotoxicity evaluation appropriate for human hazard evaluation. Molecular analysis of the *TK*-mutants may help us understand the genotoxic mechanism of MCLR [18,19].

2. Materials and methods

2.1. Cells culture and chemical treatment

The TK6 human lymphoblastoid cell line has been described previously [18]. Cells were grown in RPMI1640 medium (Gibco-BRL, Life technology Inc., Grand Island, NY) supplemented with 10% heat-inactivated horse serum (JRH Biosciences, Lenexa, KS), 200 μg/ml sodium pyruvate, 100 unit/ml penicillin, and 100 μg/ml streptomycin. The cultures were incubated at 37 °C in a 5% CO_2 atmosphere with 100% humidity and maintained at densities ranging from 10^5 to 10^6 cells/ml.

MCLR (Cas.# 101043-37-2) was purchased from Wako Pure Chemical Co. (Tokyo, Japan) and dissolved in phosphate-buffered saline just before use. Prior to their exposure, the cells were cultured in CHAT (10 μM deoxycytidine, 200 μM hypoxanthine, 0.1 μM aminopterin, 17.5 μM thymidine) medium for 2 days to reduce the background mutant fraction. Cultures of 20 ml at 5.0×10^5 cells/ml and of 50 ml at 2.0×10^5 cells/ml were treated at 37 °C with serial dilution of MCLR for 4 h and 24 h, respectively. They were then washed once, re-suspended in fresh medium, and cultured in new flasks for the MN assay and *TK* gene mutation assay, or diluted to be plated for survival estimates.

2.2. MN assay

Forty-eight hours after exposure, the MN assay samples were prepared as previously reported [20]. Briefly, approximately 10^6 cells suspended in hypotonic KCl solution were incubated for 10 min at room temperature, fixed twice with ice-cold fixative (glacial acetic acid: methanol, 1:3), and then re-suspended in methanol containing 1% acetic acid. A drop of the suspension was placed on a clean glass slide and air-dried. The cells were stained with 40 μg/ml acridine orange solution and immediately observed with the aid of an Olympus model BX50 fluorescence microscope equipped with a U-MWBV band pass filter. At least 1000 intact interphase cells for each treatment were examined, and the cells containing MN were scored.

2.3. TK gene mutation assay

The TK6 cell cultures were maintained for 3 days after exposure to permit expression of the *TK* deficient phenotype. To isolate the *TK* deficient mutants, we seeded cells into 96-well microwell plates at 40,000 cells/well in the presence of 3.0 μg/ml trifluorothymidine (TFT). Cells from each culture were also plated at 1.6 cells/well in the absence of TFT for the determination of plating efficiency (PE). All plates were incubated for 14 days at 37 °C in a 5% CO_2, humidified incubator, and then scored for colony formation. Plates containing TFT were then re-fed with TFT, incubated for an additional 14 days, and scored for the appearance of slow-growing *TK* mutants. Mutation frequencies were calculated according to the Poisson distribution [21].

2.4. LOH analysis of TK mutants

Genomic DNA was extracted from *TK* mutant cells and used as a template for PCR. The PCR-based LOH analysis at human *TK* gene was described previously [19]. Two sets of primers were used to amplify the parts of exons 4 and 7 of the *TK* gene containing frameshift mutations. Another primer set for amplifying parts of the β-globin was also prepared. Quantitative-multiple PCR was subjected to co-amplification of the three regions and qualify and quantify the PCR products. They were analyzed with an ABI310 genetic analyzer (PE Biosystems, Chiba, Japan), and classified them into non-LOH, hemizygous LOH, or homozygous LOH mutants.

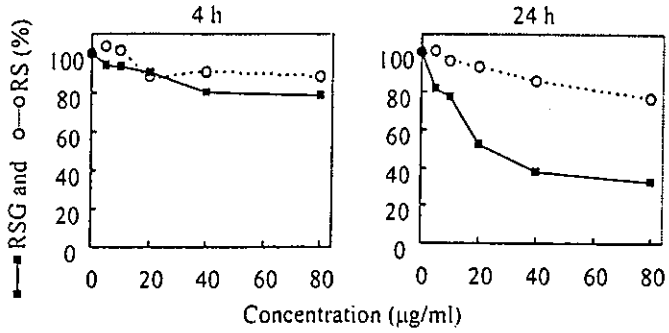

Fig. 1. Cytotoxic responses represented by RS and relative cell growth (RSG) of TK6 cells treated with MCLR for 4 or 24 h.

3. Results

3.1. Cytotoxic response to MCLR

TK6 cells were exposed to various doses of MCLR for 4 or 24 h. Fig. 1 shows cytotoxic responses; relative survival (RS) and relative suspension growth (RSG), which is relative cell growth during 72 h after exposure. Exposure to MCLR for 4 h did significantly affect RS or RSG. Exposure for 24 h, however, decreased RSG concentration-dependently, but did not significantly alter RS.

3.2. Genotoxic responses to MCLR

Exposure to MCLR for 24 h induced both MN and *TK* mutation in a concentration-dependent manner (Fig. 2). The maximum induction of MN and *TK* mutations were 4.8- and 5.1-times the control values. Two distinct phenotypic classes of *TK* mutants were generated. Normally growing (NG) mutants grew at the same rate as the wild type cells (doubling time 13–17 h), and slowly growing (SG) mutants grew at a slower rate (doubling time >21 h). NG mutants result mainly from intragenic mutations, while SG mutants result from gross genetic changes beyond the *TK* gene. The proportion of SG mutants increased in MCLR induced mutants, suggesting that MCLR was clastogenic.

3.3. Molecular analysis of TK mutants

Spontaneously arising and MCLR-induced *TK* mutants were isolated independently. The MCLR-induced

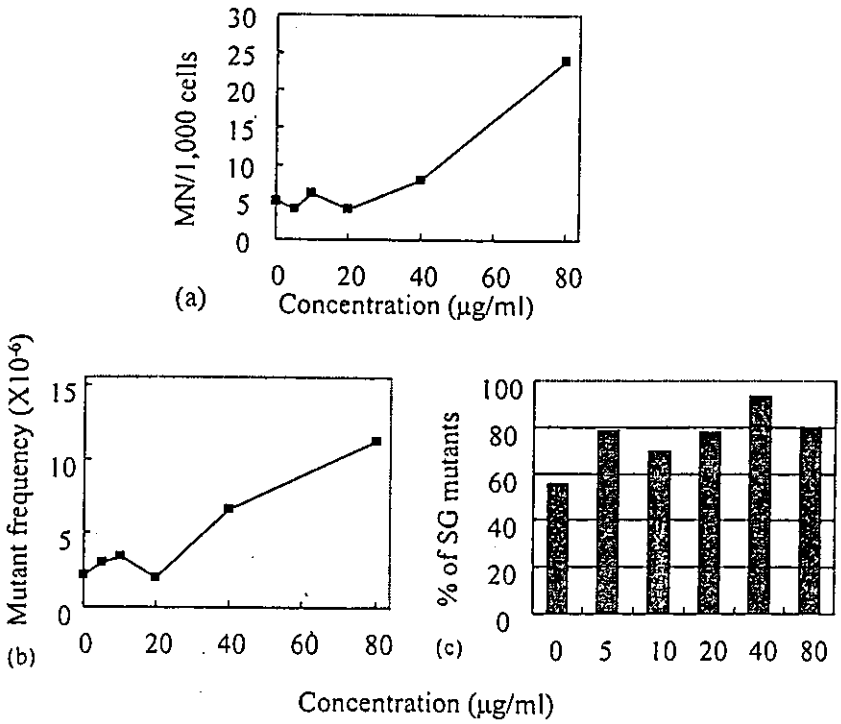

Fig. 2. MN induction (a), mutation frequency at *TK* locus (b), and percentage of slowly growing (SG) mutants (c) among TK-deficient mutants treated with MCLR for 24 h.

Table 1
Cytotoxic and mutational response to MCLR[a] and LOH analysis of TK-mutants

Treatment	Cytotoxic and mutational response			LOH analysis at *TK* gene			
	RSG (%)	MF ($\times 10^{-6}$)	% SG	No. analyzed	None LOH	Hemizygous LOH	Homozygous LOH
Spontaneous	100	2.19	56	56			
NG mutants				19	14 (74)	3 (16)	2 (11)
SG mutants				37	0 (0)	9 (24)	28 (76)
MCLR-induced	32.6	11.2	80	36			
NG mutants				9	4 (44)	5 (56)	0 (0)
SG mutants				27	0 (0)	10 (37)	17 (63)

[a] 80 μg/ml for 24 h.

mutants were produced by the treatment at 80 μg/ml for 24 h. The cytotoxicity (RSG), mutation frequency, and proportion of SG mutants by the treatment are shown in Table 1. We used PCR-based LOH analysis of genomic DNA from *TK* mutants to classify the mutants into 3 types; Non-LOH, hemizygous LOH, and homozygous LOH. We analyzed 58 spontaneous and 36 MCLR induced *TK* mutants, including NG and SG type (Table 1). Every SG mutant was a result of LOH regardless of the treatment, suggesting that SG mutants were always associated with gross genetic changes. Among the MCLR-induced mutants, 56% of NG mutants and 100% of SG mutants exhibited LOH. Every LOH in the NG mutants was hemizygous, and 63% of LOH in the SG mutants was homozygous. This is in contrast to spontaneous *TK* mutants, where the majority of spontaneous NG and SG mutants were non-LOH (74%) and homozygous LOH (76%), respectively. Fig. 3 shows the spectra of spontaneous and MCLR-induced *TK* mutants in TK6 cells, which were adjusted by considering % SG mutants. These data clearly indicate that MCLR induced LOH, but not point mutation or other small genetic changes.

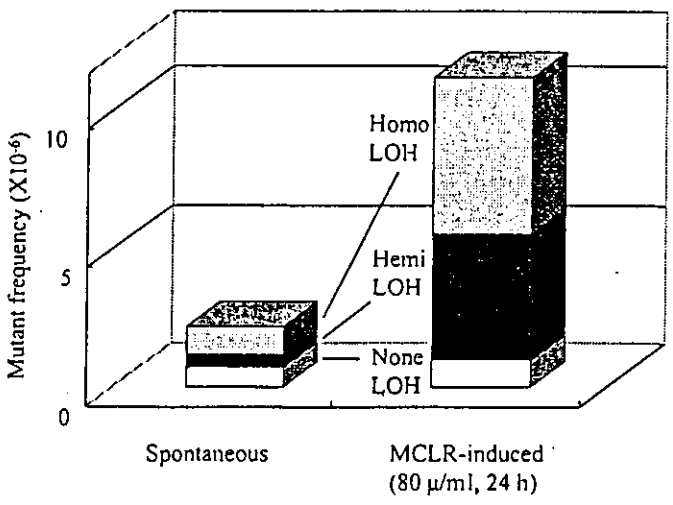

Fig. 3. Frequency and spectra of *TK* mutations in spontaneous and MCLR (80 μg/ml, 24 h) induced *TK* mutants in TK6 cells. The fraction of each mutational event was calculated by considering the ratio of NG and SG mutants and the result of molecular analysis (Table 1).

4. Discussion

Although MCLR causes severe hepatoxoxicity in mammals [9–12], its genotoxicity and carcinogenicity are inconclusive. Ding et al. [13] reported that microcystic cyanobacteria extract (MCE) significantly induced mutations in the Ames assay regardless of metabolic activation, although pure MCLR did not. Tsuji et al. [22,23] also failed to demonstrate MCLR genotoxicity in the Ames assay. On the other hand, MCLR has some genotoxic effects in mammalian cells. Ding et al [13] observed DNA damage in primary rat hepatocytes in comet assay, and Rao and Bhattacharya [14] found that MCLR could induce DNA fragmentation and strand breaks in mouse liver in vivo. Two studies reported the induction of chromosome aberrations and gene mutations in mammalian cells [15,24].

Our present study clearly demonstrated the in vitro genotoxicity of MCLR, which induced MN formation as well as gene mutations in human cells. A 24 h treatment was required, however, to express the effects. Although MCLR is toxic and highly lethal to

mice in vivo, it seems less toxic in vitro, particularly in non-liver cells. That may be because cyclic heptapeptide microcystines do not generally penetrate most cells including bacteria, and a specific transport system may be required [25]. We used 2 parameters to estimate MCLR cytotoxicty—RS and RSG. RS is relative plating efficiency just after exposure, while RSG is relative cell growth for the 3 days following exposure. RSG exhibited stronger response than RS, suggesting that MCLR has an inhibitory effect on cell growth [26]. Because the cytotoxicity was not severe, the genotoxic responses to MCLR must have been due to physiological effects. In the *TK* gene mutation assay, MCLR elevated not only the frequency of mutants, but also the fraction of SG mutants, suggesting that MCLR induced predominantly gross structural changes, such as large deletions, recombinations, and rearrangements.

Molecular analysis strongly supported this hypothesis. Most of the *TK* mutants induced by MCLR were the result of LOH, while the fraction of non-LOH mutants hardly changed (Fig. 3). LOH is an important genetic event in tumorigenesis and is frequently observed in a variety of human tumors. The two major mechanisms for generating LOH are deletion (hemizygous LOH) and inter-allelic recombination (homozygous LOH) [18,19]. Both mechanisms involve the repair of chromosomal double strand breaks (DSBs), either non-homologous end-joining and homologous recombination (HR), although their regulation and role have not been clarified [27]. Other mechanisms may be involved, too, including illegitimate recombination and mitotic non-disjunction [26]. DSB-inducing agents, such as ionizing irradiations, effectively produce LOH mutations through the repair pathways [17,18]. MCLR clastogenic activity may also involve DSBs. Honma and Little [28] demonstrated that 12-*O*-tetradecanoyl-phorbol-13-acetate (TPA), which is the most active tumor promoter known, preferably induces homozygous LOH through HR. MCLR also has tumor promoting activity; like the tumor promoter Okadaic acid, it inhibits protein phosphatase types 1 and 2A [29]. A cyanobacterial toxin, nodularin, which also inhibits protein phosphatases 1 and 2A with the same potency as does MCLR has been recognized as rat liver carcinogen rather than a tumor promoter [30]. The genotoxicity of nodularin, however, has not been clear. Matsushima et al. [31] demonstrated that MCLR promotes rat liver cancer initiated with diethyl-nitrosamine. The tumor promoting activity of MCE has been also shown in a two-stage transformation assay in vitro using Syrian hamster embryonic cells [32]. The induction of LOH by MCLR through recombination may be associated with its tumor promoting activity. It is reported that Okadaic acid induces minisatellite mutation in NIH3T3 cells probably through recombination events [33]. The potent hepatocarcinogen aflatoxin B1 also preferably induces LOH through HR in TK6 cells and mouse lymphoma L5178Y cells [34,35].

In conclusion, MCLR was clastogenic in human cells in the present study. It induced LOH, but not point mutations. The genotoxic activity may have been associated with the inductions of DSBs and/or its promoting activity. The association between a high incidence of primary liver cancer and drinking of pond and ditch water polluted by high level of cyanobacteria producing MCLR [3,36,37] suggests that liver is a target organ for MCLR carcinogenisity. Further studies using liver cells and tissues are required to clarify the mechanisms of MCLR genotoxicity in the liver.

Acknowledgements

This study was supported by a grant from the Japan–China Sasagawa Medical Fellowship.

References

[1] W.W. Carmichael. Toxins of freshwater algae. In: A.T. Tu (Ed.), Handbook of natural Toxins. Marcel Dekker, New York, 1988, pp. 121–147.
[2] G.A. Codd, S.G. Bell, P. Brooks, Cyanobacterial toxins in water, Water Sci. Technol. 21 (1989) 1–13.
[3] W.W. Carmichael, The toxins of cyanobacteria, Sci. Am. 270 (1994) 78–86.
[4] F.D. Galey, V.R. Beasley, W.W. Carmichael, G. Kleppe, S. Hooser, W.M. Haschek, Blue-green algae (*Microcysis aeruginosa*) hepatotoxicosis in dairy cows, Am. J. Vet. Res. 48 (1987) 1415.
[5] I.R. Falconer, A.M. Bersfoed, M.T.C. Runnegar, Evidence of liver damage by toxin from a bloom of blue-green algae, *Microcystis aeruginosa*, Med. J. Aust. 1 (1983) 511–514.
[6] I.R. Falconer, Effects on human health of some toxic cyanobacteria (blue-green algae) in reservoirs, Toxicity Assess. 4 (1989) 175–184.
[7] W.P. Brooks, G.A. Codd, Distribution of *Microcystis aeruginosa* peptide toxin and interactions with hepatic microsomes in mice, Pharmacol. Toxicol. 60 (1987) 187–191.

[8] A.S. Dabholker, W.W. Carmichael, Ultrastructural changes in the mouse liver induced by hepatotoxin from the freshwater cyanobacterium Microcystis aeruginosa strain 7820, Toxicon 25 (1987) 285–292.
[9] G.A. Codd, S.G. Bell, P. Brooks, Cyanobacterial toxins in water, Water Sci. Technol. 21 (1989) 1–13.
[10] S.B. Hooser, V.R. Beasley, R.A. Lovell, W.W. Carmichael, W.M. Haschek, Toxicity of microcystin-LR, a cyclic heptapeptide hepatotoxin from *Microcystis aeruginosa* to rats and mice, Vet. Pathol. 26 (1989) 246–252.
[11] P.V. Rao, R. Bhattacharya, S.C. Pant, A.S.B. Bhaskar, Toxicity evaluation of in vitro cultures of freshwater cyanobacterium *Microcystis aeruginosa*. Part 1. Hepatotoxic and histopathological effects in rats, Biomed. Environ. Sci. 8 (1995) 254–264.
[12] R. Bhattacharya, P.V.L. Rao, A.S.B. Bhaskar, S.C. Pant, S.N. Dube, Liver slice culture for assessing hepatotoxicity of freshwater cyanobacteria, Hum. Exp. Toxicol. 15 (1996) 105–110.
[13] W.X. Ding, H.M. Shen, H.G. Zhu, B.L. Lee, C.N. Ong, Genotoxicity of microcystic cyanobacteria extract of a water source in China, Mutation Res. 442 (1999) 69–77.
[14] P.V. Rao, R. Bhattacharya, The cyanobacteral toxin microcystin-LR induced DNA damage in mouse liver in vivo, Toxicology 114 (1996) 29–36.
[15] H. Suzuki, M.F. Watanabe, Y. Wu, T. Sugita, K. Kita, T. Sato, X.L. Wang, H. Tanzawa, S. Sekiya, N. Suzuki, Mutagenicity of microcystin-LR in human RSa cells, Int. J. Mol. Med. 2 (1998) 109–112.
[16] H.L. Liber, W.G. Thilly, Mutation assay at the thymidine kinase locus in diploid human lymphoblasts, Mutat. Res. 94 (1982) 467–485.
[17] C.Y. Li, D.W. Yandell, J.B. Little, Molecular mechanism of spontaneous and induced loss of heterozygosity in human cells in vitro, Somat. Cell Mol. Genet.18 (1992) 77–87.
[18] M. Honma, M. Hayashi, T. Sofuni, Cytotoxic and mutagenic responses to X-rays and chemical mutagens in normal and p53-mutated human lymphoblastoid cells, Mutat. Res. 374 (1997) 89–98.
[19] M. Honma, M. Momose, H. Tanabe, H. Sakamoto, Y. Yu, J.B. Little, T. Sofuni, M. Hayashi, Requirement of wild-type p53 protein for maintenance of chromosomal integrity, Mol. Carcinogenesis 28 (2002) 203–214.
[20] L.S. Zhang, M. Honma, A. Matsuoka, T. Suzuki, T. Sofuni, M. Hayashi, Chromosome painting analysis of spontaneous and methylmethanesulfonate, induced trifluorothymidine-resistant L5178Y cell colonies, Mutat. Res. 370 (1996) 181–190.
[21] E.E. Furth, W.G. Thilly, B.W. Penman, H.L. Liber, W.M. Rand, Quantitative assay for mutation in diploid human lymphoblasts using microtiter plates, Anal. Biochem. 110 (1981) 1–8.
[22] K. Tsuji, T. Watanuki, F. Kondo, M.F. Watanabe, S. Suzuki, H. Nakazawa, H. Uchida, K.I. Harada, Stability of microcystins from cyanobacteria—II. Effect of UV light on decomposition and isomerization, Toxicon 33 (1995) 1619–1631.
[23] K. Tsuji, T. Watanuki, F. Kondo, M.F. Watanabe, H. Nakazawa, S. Suzuki, H. Uchida, K.I. Harada, Stability of microcystins from cyanobacteria. Part IV. Effect of chlorination on decomposition, Toxicon 35 (1997) 1033–1041.
[24] W.M. Repavich, W.C. Sonzongni, J.H. Standridge, R.E. Wedephohl, L.F. Meisner, Cyanobacteria (blue-green algae) in Wisconsin waters: acute and chronic toxicity, Water Res. 24 (1990) 225–231.
[25] M. Runnegar, N. Berndt, N. Kaplowitz, Microcystin uptake and inhibition of protein phosphatases: effects of chemoprotectants and self-inhibition in relation to known hepatic transporters, Toxicol. Appl. Pharmacol. 134 (1995) 264–272.
[26] M. Honma, M. Momose, H. Sakamoto, T. Sofuni, M. Hayashi, Spindle poisons induce allelic loss in mouse lymphoma cells through mitotic non-disjunction, Mutat. Res. 493 (2001) 110–114.
[27] J.M. Stark, M. Jasin, Extensive loss of heterozygosity is suppressed during homologous repair of chromosomal breaks, Mol. Cell. Biol. 23 (2003) 733–743.
[28] M. Honma, J.B. Little, Recombinagenic activity of the phorbol ester 12-O-tetradecanoylphorbol-13-acetate in human lymphoblastoid cells, Carcinogenesis 16 (1995) 1717–1722.
[29] S. Yoshizawa, R. Matsushima, M.F. Watanabe, K.I. Harada, W.W. Carmichael, H. Fujiki, Inhibition of protein phosphatases by microcystins and nodularin associated with hepatotoxicity, J. Cancer Res. Clin. Oncol. 116 (1990) 609–614.
[30] T. Ohta, E. Sueoka, N. Iida, A. Komori, M. Suganuma, R. Nishiwaki, M. Tatematsu, S.J. Kim, W.W. Carmichael, H. Fujiki, Nodularin, a potent inhibitor of protein phosphatases 1 and 2A, is a new environmental carcinogen in male F344 rat liver, Cancer Res. 54 (1994) 6402–6406.
[31] R. Matsushima, T. Ohta, S. Nishiwaki, M. Suganuma, K. Koyama, T. Ishikawa, W.W. Carmichael, H. Fujiki, Liver tumor promotion by the cyanobacterial cyclic peptide toxin microcystin-LR, J. Cancer Res. Clin. Oncol. 118 (1992) 420–424.
[32] H.B. Wang, H.G. Zhu, Promoting activity of microcystins extract from waterblooms in SHE cell transformation assay, Biomed. Environ. Sci. 9 (1996) 46–51.
[33] H. Nakagama, S. Kaneko, H. Shima, H. Inamori, H. Fukuda, R. Kominami, T. Sugimura, M. Nagao, Induction of minisatellite mutation in NIH 3T3 cells by treatment with the tumor promoter okadaic acid, Proc. Natl. Acad. Sci. U.S.A. 94 (1997) 10813–10816.
[34] P.M. Stettler, C. Sengstag, Liver carcinogen aflatoxin B1 as an inducer of mitotic recombination in a human cell line, Mol. Carcinogen 31 (2001) 125–138.
[35] V. Preisler, W.J. Caspary, F. Hoppe, R. Hagen, H. Stopper, Aflatoxin B1-induced mitotic recombination in L5178Y mouse lymphoma cells, Mutagenesis 15 (2000) 91–97.
[36] S.Z. Yu, G. Chen, Blue-green algae toxins and liver cancer, Chin. J. Cancer Res. 6 (1994) 9–17.
[37] Y. Ueno, S. Nagata, T. Tsutsumi, A. Hasegawa, M.F. Watanabe, H.D. Park, G.C. Chen, G. Chen, S.Z. Yu, Detection of microcystins, a blue-green algal hepatotoxin, in drinking water sampled in Haimen and Fusui, endemic areas of primary liver cancer in China, by highly sensitive immunoassay, Carcinogenesis 17 (1996) 1317–1321.

Available online at www.sciencedirect.com
SCIENCE DIRECT
Biochimica et Biophysica Acta 1688 (2004) 137–144
BIOCHIMICA ET BIOPHYSICA ACTA
BBA
www.bba-direct.com

The absence of a functional relationship between ATM and BLM, the components of BASC, in DT40 cells

Wensheng Wang[a,b,1], Masayuki Seki[a,*], Makoto Otsuki[a], Shusuke Tada[a], Noriaki Takao[c], Ken-ichi Yamamoto[c], Makoto Hayashi[b], Masamitsu Honma[b], Takemi Enomoto[a]

[a] *Molecular Cell Biology Laboratory, Graduate School of Pharmaceutical Sciences, Tohoku University, Sendai 980-8578, Japan*
[b] *Division of Genetics and Mutagenesis, National Institute of Health Sciences, 1-18-1, Kamiyoga, Setagaya, Tokyo 158-8501, Japan*
[c] *Department of Molecular Pathology, Cancer Research Institute, Kanazawa University, Kanazawa 920-0934, Japan*

Received 3 May 2002; received in revised form 11 November 2003; accepted 12 November 2003

Abstract

Bloom syndrome (BS) and ataxia-telangiectasia (A-T) are rare autosomal recessive diseases associated with chromosomal instability. The genes responsible for BS and A-T have been identified as *BLM* and *ATM*, respectively, whose products were recently found to be components of BRCA1-associated genome surveillance complex (BASC), a supercomplex possibly involved in the recognition and repair of aberrant DNA structures. Based on experiments using $BLM^{-/-}$ DT40 cells and $BLM^{-/-}/RAD54^{-/-}$ DT40 cells, we previously suggested that BLM functions to reduce the formation of double-strand breaks (DSBs) during DNA replication. To examine whether ATM is involved in the recognition and/or repair of DSBs generated in $BLM^{-/-}$ DT40 cells and to address the functional relationship between the two BASC components, we generated $BLM^{-/-}/ATM^{-/-}$ DT40 cells and characterized their properties as well as those of $ATM^{-/-}$ and $BLM^{-/-}$ DT40 cells. $BLM^{-/-}/ATM^{-/-}$ cells proliferated slightly more slowly than either $BLM^{-/-}$ or $ATM^{-/-}$ cells. The sensitivity of $BLM^{-/-}/ATM^{-/-}$ cells to γ-irradiation was similar to that of $ATM^{-/-}$ cells, while $BLM^{-/-}$ cells were slightly resistant to γ-irradiation compared with wild-type cells. $BLM^{-/-}$ cells showed sensitivity to methyl methanesulfonate (MMS) and UV irradiation while $ATM^{-/-}$ cells did not show sensitivity to either agent. The sensitivity of $BLM^{-/-}/ATM^{-/-}$ cells to MMS and UV was similar to that of $BLM^{-/-}$ cells. Disrupting the function of ATM reduced the targeted integration frequency in $BLM^{-/-}$ DT40 cells. However, a defect in ATM only slightly reduced the increased sister chromatid exchanges (SCEs) in $BLM^{-/-}$ DT40 cells.

Keywords: BLM; ATM; BASC; Targeted integration; SCE; DSB

1. Introduction

Bloom syndrome (BS) is a rare autosomal recessive disease characterized by immunodeficiency, retarded growth, male sterility, sensitivity to sunlight, and a predisposition to a wide variety of cancers. Cells derived from BS patients exhibit elevated frequencies of sister chromatid exchanges (SCEs), chromosomal breaks, and interchanges between homologous chromosomes [1]. However, they show a retarded rate of elongation of nascent DNA chains [2] and accumulate abnormal replication intermediates [3]. In addition, immunodepletion of *Xenopus* Bloom syndrome gene product (xBLM) from a *Xenopus* egg extract severely inhibited the replication of chromosomal DNA in reconstituted nuclei and the inhibition was cancelled by the addition of recombinant xBLM [4]. Thus, BLM seems to be somehow involved in DNA replication.

Ataxia-telangiectasia (A-T) is also a rare autosomal recessive disease displaying chromosome instability. Symptoms of A-T include cerebella ataxia, oculocutaneous telangiectasia, immunodeficiency, premature aging, predisposition to lymphoid malignancy, and radiosensitivity. Cells derived from A-T patients show high levels of chromosome aberrations and hypersensitivity to ionizing radiation [5]. The product of the gene responsible for A-T, ATM, is a member of the family of phosphoinositide kinases [6]. ATM plays essential roles in the recognition, signaling and repair of DNA damage, especially DNA double-strand breaks (DSBs). ATM is an upstream factor of p53 and

* Corresponding author. Tel.: +81-22-217-6874; fax: +81-22-217-6873.
E-mail address: seki@mail.pharm.tohoku.ac.jp (M. Seki).
[1] Present address: Department of Biochemistry and Biophysics, University of Rochester Medical Center, Rochester, NY 14642, USA.

0925-4439/$ - see front matter © 2003 Elsevier B.V. All rights reserved.
doi:10.1016/j.bbadis.2003.11.008

regulates progression of the cell-cycle and apoptosis by phosphorylating p53 [7,8]. ATM also interacts with and phosphorylates c-Abl, which interacts with p53, induces apoptosis and arrests cells in G1 phase after ionizing radiation [9,10]. Chk2 is also phosphorylated by ATM and regulates progression of the cell cycle through p53-dependent and independent pathways [11–13].

Recently, BLM and ATM have been reported to be components of BRCA1-associated genome surveillance complex (BASC), a supercomplex supposed to be involved in the recognition and repair of aberrant DNA structures, which consists of BRCA1, MSH2, MSH6, MLH1, RFCs, and RAD50 as well as BLM and ATM [14]. In addition, BLM is phosphorylated by ATM in response to ionizing radiation [15]. However, the functional relationship between BLM and the other components of BASC is not clear at present.

It has been reported that DSBs are produced by cleavage of the Holliday junctions which are formed by the annealing of two newly synthesized DNA at arrested replication forks [16]. The gene responsible for BS encodes a protein which is a member of the RecQ helicase family and actually has DNA helicase activity [17,18]. In addition, BLM selectively binds and acts on Holliday junctions to promote branch migration over an extended length of DNA [19]. In our previous study using *BLM*$^{-/-}$ cells constructed from a chicken B cell line, DT40 and *BLM*$^{-/-}$/*RAD54*$^{-/-}$ DT40

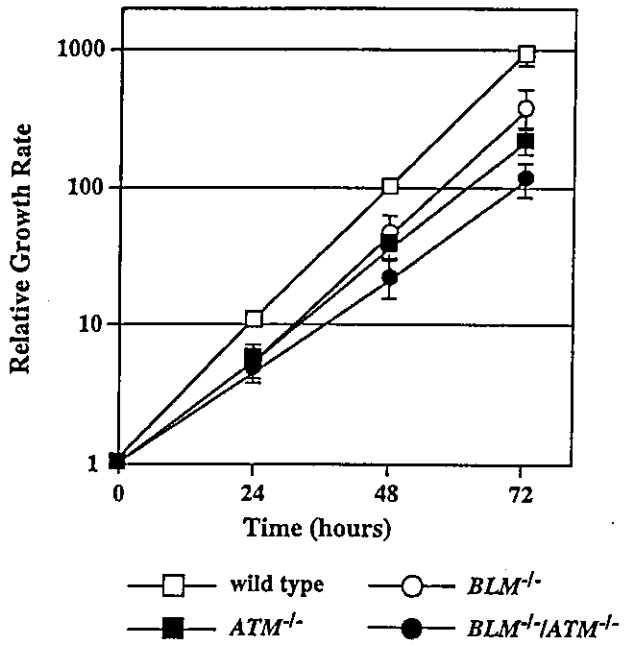

Fig. 2. Growth curves of wild-type, *ATM*$^{-/-}$, *BLM*$^{-/-}$ and *BLM*$^{-/-}$/*ATM*$^{-/-}$ DT40 cells. Wild-type, *ATM*$^{-/-}$, *BLM*$^{-/-}$ and *BLM*$^{-/-}$/*ATM*$^{-/-}$ DT40 cells were inoculated into 35 mm dishes, and enumerated at the time indicated. Three independent experiments were performed and typical data were presented. Error bars show the standard deviation of the mean.

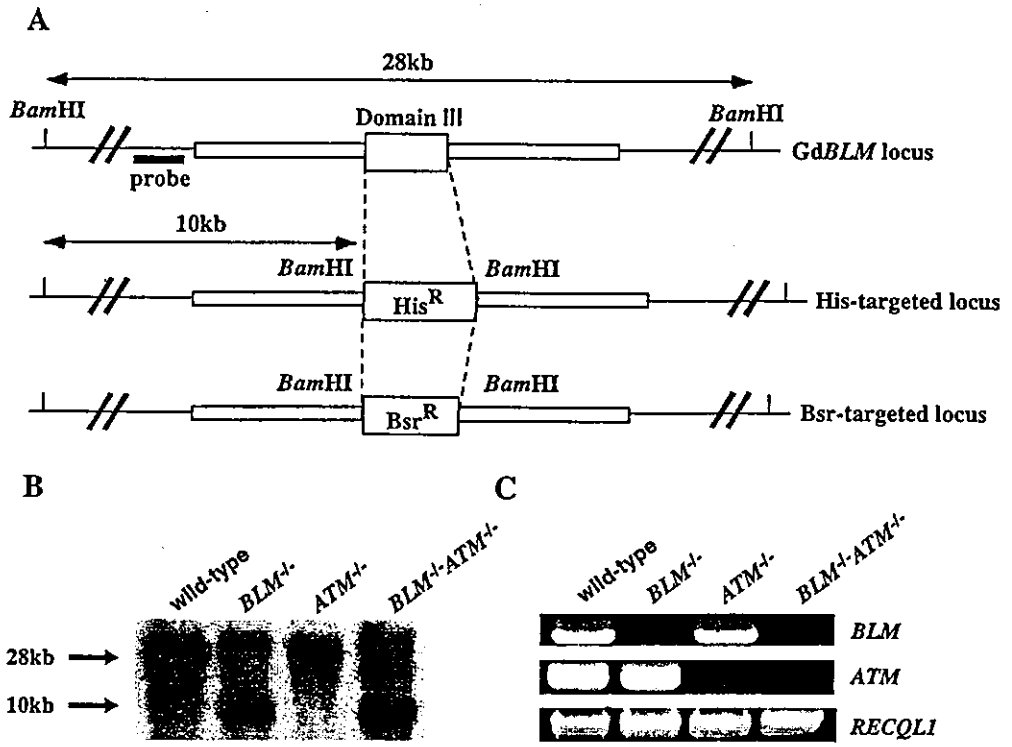

Fig. 1. Generation of DT40 *BLM*$^{-/-}$/*ATM*$^{-/-}$ double mutant cells. (A) Schematic representation of part of the *BLM* genomic locus, targeting constructs, and the configuration of the targeted locus. (B) Southern blot analyses for wild-type (+/+), *BLM*$^{-/-}$, *ATM*$^{-/-}$, and *BLM*$^{-/-}$/*ATM*$^{-/-}$ cells were carried out to confirm the *BLM* gene disruption in putative *BLM*$^{-/-}$/*ATM*$^{-/-}$ cells. *Bam*HI-digested genomic DNA was hybridized with the probe shown in panel A. (C) RT-PCR analysis of total RNA from wild-type (+/+), *BLM*$^{-/-}$, *ATM*$^{-/-}$, and *BLM*$^{-/-}$/*ATM*$^{-/-}$ cells. The primer sets used to detect *ATM*, *BLM*, and *RECQL1* (control) were described in Materials and methods.

cells, we suggested that the physiological function of BLM is to resolve Holliday junctions formed during DNA replication, and DSBs formed due to a defect in BLM function are repaired mainly by homologous recombination, resulting in an increased incidence of SCE [20]. However, the precise mechanism of the formation of SCE is not known. Interestingly, most of the components of BASC, such as BRCA1, MSH2, RAD50, and ATM, are known to be somehow involved in homologous recombination [14].

In this study, to examine whether ATM is involved in the formation of SCE in *BLM*$^{-/-}$ DT40 cells and to elucidate the functional relationship between the two BASC components, BLM and ATM, under DNA damage-induced conditions, we generated *BLM*$^{-/-}$/*ATM*$^{-/-}$ double gene-disrupted DT40 cells and characterized their properties as well as those of *BLM*$^{-/-}$ and *ATM*$^{-/-}$ DT40 cells.

2. Materials and methods

2.1. Construction of targeting vectors

Chicken *BLM*-targeting constructs, *BLM*-histidinol® and *BLM*-blasticidin S®, were made as described previously [20].

2.2. Cell culture and DNA transfection

The cell culture conditions were described previously [20]. *BLM*$^{-/-}$ and *ATM*$^{-/-}$ DT40 cells were generated as reported elsewhere [20,21]. To generate *BLM*$^{-/-}$/*ATM*$^{-/-}$ DT40 cells, *ATM*$^{-/-}$ DT40 cells were electroporated with 30 μg of linearized *BLM*-targeting constructs using a Gene Pulser II apparatus (BioRad, Hercules, CA, USA) at 550 V and 25 μF. Drug-resistant colonies were selected in 96-well plates with medium containing 1 mg/ml of histidinol or 20 μg/ml of blasticidin S. Gene disruption was confirmed by Southern blotting and RT-PCR. Primer sets used to detect *ATM*, *BLM*, and *RECQL1* (control) by RT-PCR are as follows:

ATM-sense:5′-GTGGATCCCACAGGAAGATA-3′
ATM-antisense: 5′-GTCAGCTTCATCCTCTGGTC-3′
BLM-sense: 5′-ACCAGCGTGTGTCTCTGCTG-3′
BLM-antisense: 5′-CTACAGATTTTGGAAGGGAAGC-3′
RECQL1-sense: 5′-ATGACAGCTGTGGAAGTGCTA-3′
RECQL1-antisense: 5′-TCAGTCAAGAACAA-CAGGTTGGTCATCTC-3′.

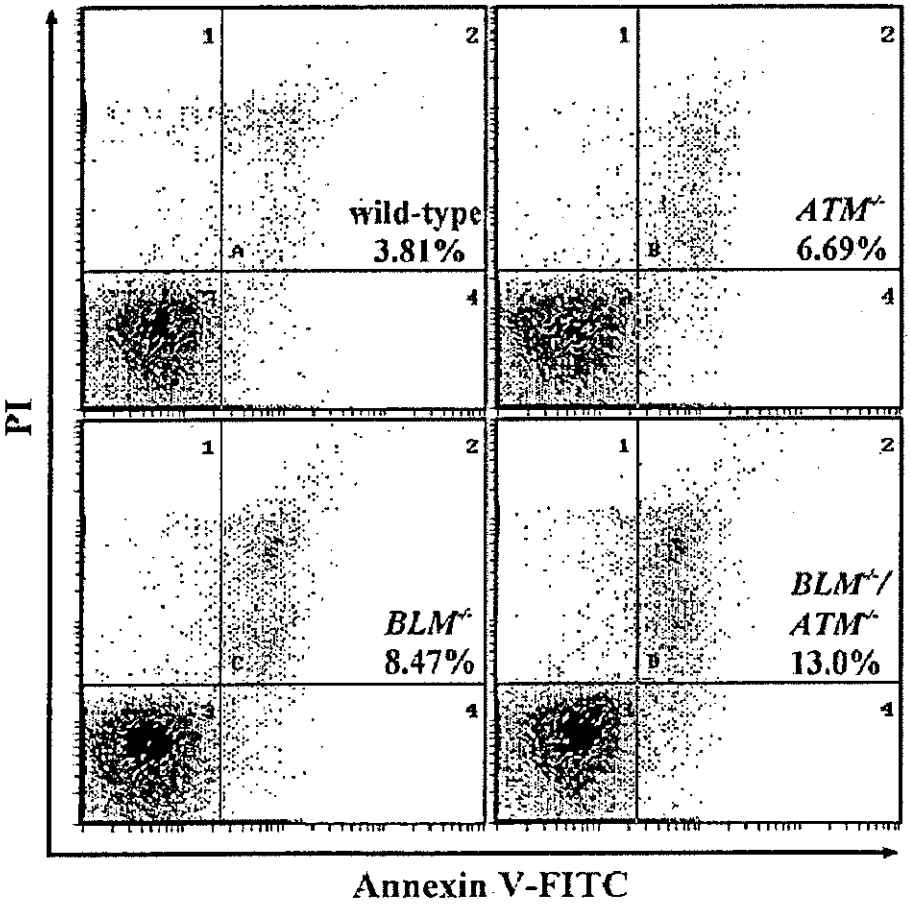

Fig. 3. Flow cytometry for detection of dead cells. Cells (5×10^5) were treated according to the Manual of the ApoAlert Annexin V-FITC Apoptosis kit and 3×10^4 cells were analyzed by Flow Cytometry. The number in the upper right corner indicates the percentage of dead cells.

2.3. Growth curve and flow cytometry

Cells (2×10^4) were inoculated and cultured at 39 °C for specified periods. They were then enumerated with a Particle Count and Size Analyzer (Coulter, USA) and relative growth rates were estimated. The cell cycle distribution pattern and cell death were examined with a EPICS XL Flow Cytometer (Coulter) after treatment according to the manual of the BrdU Flow Kit (Beckon Dickinson, CA) and ApoAlert Annexin V-FITC Apoptosis Kit (Clontech Laboratories, Inc., CA).

2.4. Measurements of MMS, UV and γ-radiation sensitivity

The sensitivity to methyl methanesulfonate (MMS) was evaluated as described previously [20]. To determine the sensitivity to UV or ionizing radiation, cells were irradiated with UV light or γ-rays at given doses, and then inoculated into dishes containing growth medium supplemented with 1.5% methylcellulose. The colonies were enumerated 9 days after inoculation. Survival was determined by comparing results with the number of colonies of untreated cells.

2.5. Measurements of targeted integration frequency and SCE frequency

To analyze targeted integration events at the chicken RECQL1, RECQL5 and RAD54 loci, a targeting construct, either chicken RECQL1-Hygromycin®, RECQL5-Hygromycin® or RAD54-Hygromycin® (a gift from Dr. Takeda), was transfected into cells, and then cells were selected with the medium containing 2.5 mg/ml of hygromycin (Wako Pure Chemical Industries, Ltd. Japan). Genomic DNA of drug-resistant clones was isolated and targeted integration was confirmed by polymerase chain reaction and Southern blotting. SCE analysis was performed as described previously [22].

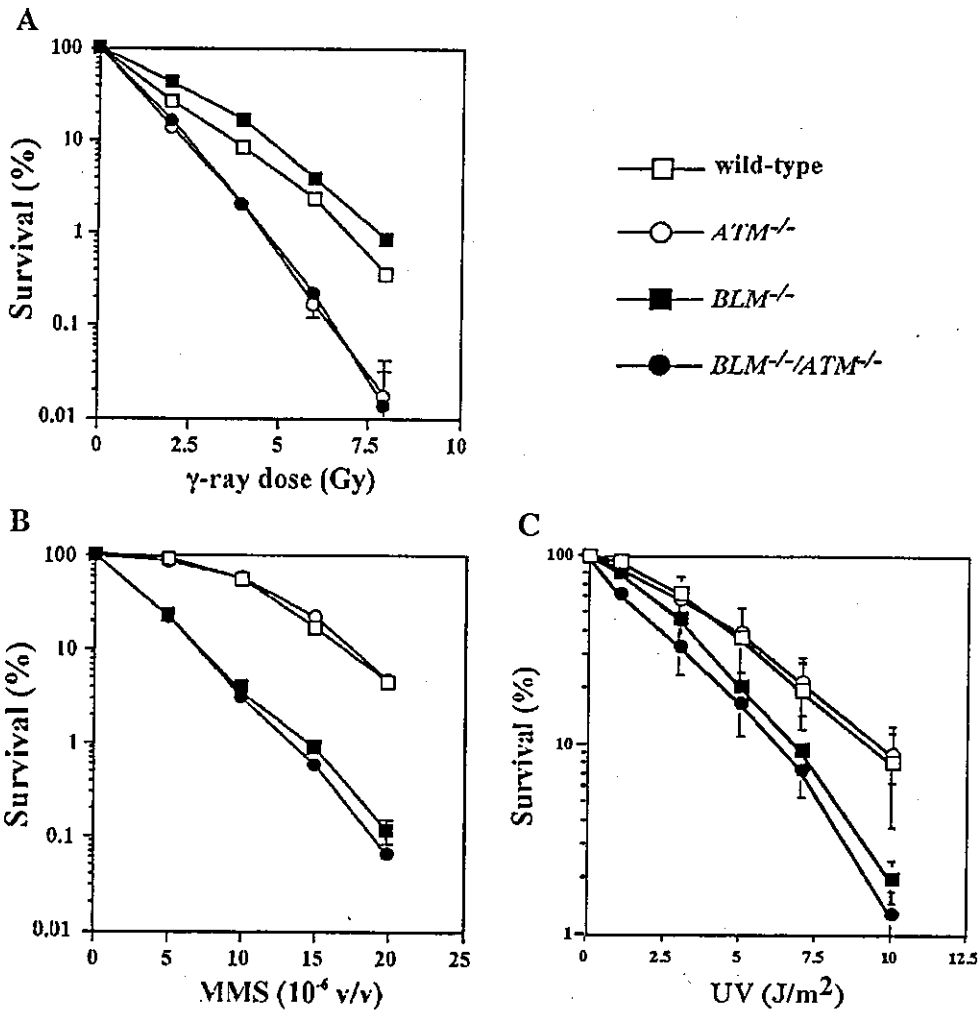

Fig. 4. Sensitivity of cells with various genotypes to γ-irradiation, MMS, and UV-irradiation. (A) γ-irradiation sensitivity, (B) MMS sensitivity, (C) UV-irradiation sensitivity. Sensitivities of wild-type, $ATM^{-/-}$, $BLM^{-/-}$, and $BLM^{-/-}/ATM^{-/-}$ DT40 cells to γ-irradiation, MMS, and UV-irradiation were determined as described under Materials and methods. Three independent experiments were performed and typical data were presented. Each value represents the mean of the survival rate and error bars show the standard deviation of the mean.

3. Results

To generate $ATM^{-/-}/BLM^{-/-}$ DT40 cells, *BLM*-histidinol® and *BLM*-blasticidin S® targeting vectors were sequentially transfected into $ATM^{-/-}$ DT40 cells (Fig. 1A) [21]. Disruption of the corresponding genes in $ATM^{-/-}/BLM^{-/-}$, $BLM^{-/-}$, and $ATM^{-/-}$ cells was confirmed by Southern blotting (Fig. 1B). In addition, we confirmed by RT-PCR the absence of *ATM* message in $ATM^{-/-}$ cells and $BLM^{-/-}/ATM^{-/-}$ cells, and the absence of *BLM* message in $BLM^{-/-}$ cells and $BLM^{-/-}/ATM^{-/-}$ cells (Fig. 1C).

We first monitored the growth curves of wild-type, $ATM^{-/-}$, $BLM^{-/-}$ and $BLM^{-/-}/ATM^{-/-}$ cells. $BLM^{-/-}/ATM^{-/-}$ cells proliferated at a lower rate than either single mutant indicating that the simultaneous defect of ATM and BLM results in an additive effect on cell proliferation (Fig. 2). To obtain an insight into the cause of the slow growth phenotype in $BLM^{-/-}/ATM^{-/-}$ DT40 cells, we investigated cell cycle distribution patterns and spontaneous cell death by flow cytometry. $BLM^{-/-}/ATM^{-/-}$ cells showed no obvious difference in cell cycle distribution (data not shown), but they showed a high rate of spontaneous cell death as compared with $ATM^{-/-}$, $BLM^{-/-}$, or wild-type cells (Fig. 3).

It has been demonstrated that ATM-deficient DT40 cells exhibit high sensitivity to ionizing irradiation [20,21]. Thus, we examined the sensitivity to γ-irradiation of $BLM^{-/-}/ATM^{-/-}$ cells as well as wild-type, $ATM^{-/-}$, and $BLM^{-/-}$ cells. As shown in Fig. 4A, the sensitivity of $BLM^{-/-}/ATM^{-/-}$ cells to γ-irradiation was similar to that of $ATM^{-/-}$ cells. In contrast to $ATM^{-/-}$ cells, $BLM^{-/-}$ cells were slightly resistant to γ-irradiation as compared with wild-type cells.

We previously reported that $BLM^{-/-}$ DT40 cells showed hypersensitivity to MMS as compared with wild-type cells [20]. Thus, we next investigated the sensitivity of $ATM^{-/-}/BLM^{-/-}$ cells to MMS. In contrast to $BLM^{-/-}$ cells, $ATM^{-/-}$ cells showed a similar sensitivity to MMS as the wild-type cells. The sensitivity of $ATM^{-/-}/BLM^{-/-}$ cells to MMS was similar to that of $BLM^{-/-}$ cells (Fig. 4B). Similar results were obtained upon exposure to ultraviolet light (Fig. 4C).

Table 1
Targeted integration frequency

Locus[a]	Targeted integration/total integration (%)			
	Wild-type	$ATM^{-/-}$	$BLM^{-/-}$	$BLM^{-/-}/ATM^{-/-}$
RECQL1	41.67 ± 0.00	37.50 ± 5.89	87.50 ± 5.89	66.67 ± 3.61*
RECQL5	37.50 ± 5.89	27.08 ± 2.95	83.33 ± 2.95	54.17 ± 7.22*
RAD54	45.83 ± 5.89	25.00 ± 0.00	95.83 ± 0.00	68.14 ± 5.01**

[a] Indicated loci were targeted by targeting constructs *RECQL1*-Hygromycin®, *RECQL5*-Hygromycin®, and *RAD54*-Hygromycin®. Results are represented as means ± S.D. of two to three experiments. Significant differences from the value of $BLM^{-/-}$ are represented by * ($P<0.05$) or ** ($P<0.01$). Statistical analysis was performed by means of Student's *t*-test.

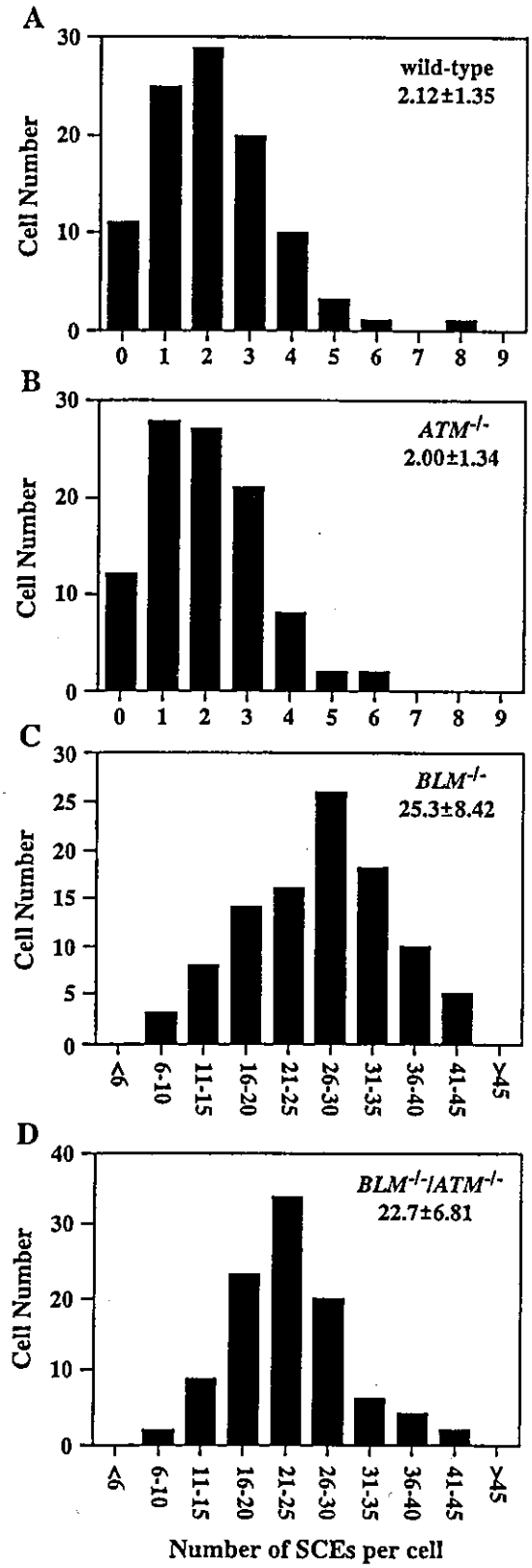

Fig. 5. Histograms of SCE in cells with various genotypes. Spontaneous SCEs in the macrosomes of 100 metaphase cells were counted. Histograms show the frequency of cells with the indicated number of SCEs per cell. The mean ± S.D. number of SCEs per cell is shown in the upper right corner.

BLM$^{-/-}$ DT40 cells showed an increased incidence of SCE and increased targeted integration frequency [20]. Thus, it is interesting to examine whether ATM is involved in the targeted integration and SCE in *BLM*$^{-/-}$ cells. As shown in Table 1, *ATM*$^{-/-}$ cells showed a slightly lower targeted integration frequency than wild-type cells as described previously [21]. The targeted integration frequencies in *BLM*$^{-/-}$/*ATM*$^{-/-}$ cells were higher than those in wild-type cells, but lower than those in *BLM*$^{-/-}$ cells, indicating that ATM is partly involved in targeted integration in *BLM*$^{-/-}$ DT40 cells.

We next analyzed frequencies of SCE in wild-type, *ATM*$^{-/-}$, *BLM*$^{-/-}$, and *BLM*$^{-/-}$/*ATM*$^{-/-}$ cells. The frequency of SCE in *ATM*$^{-/-}$ cells was almost the same as that in wild-type cells (Fig. 5A and B). The increased frequency of SCE in *BLM*$^{-/-}$ cells was only slightly decreased by the disruption of the *ATM* gene ($P<0.05$) (Fig. 5C and D), indicating a small contribution of ATM to the formation of SCE in *BLM*$^{-/-}$ DT40 cells.

4. Discussion

To our knowledge, this is the first study to genetically investigate the functional relationship between BLM and ATM, two of the components of BASC. It has been demonstrated that BLM is phosphorylated by ATM in response to ionizing radiation [15]. The sensitivity of *ATM*$^{-/-}$/*BLM*$^{-/-}$ cells to γ-irradiation was similar to that of *ATM*$^{-/-}$ cells, and *BLM*$^{-/-}$ cells showed slight resistance to γ-irradiation compared with wild-type cells. The results indicate that ATM plays an important role in the repair of DNA lesions induced by γ-irradiation as expected, while BLM has essentially no function in the repair of these lesions at least when the function is assessed based on viability. ATM is thought to be a signaling protein acting in response to DNA damage induced by ionizing radiation as a sensor. Suzuki et al. [23] have demonstrated that ATM associates with double strand DNA and the association is increased under ionizing radiation. In addition, after ionizing radiation, ATM phosphorylates the downstream proteins that are involved in DNA recombination repair [24]. In contrast, BLM is not thought to be involved directly in DNA recombination repair. Consistent with this notion, it has been indicated that a defect of BLM does not affect the formation of RAD51 foci under ionizing radiation [25,26]. Taken together, these result further support the notion that BLM functions to reduce the formation of DSBs during DNA replication [20] and is not involved in the repair of DSBs.

The slight resistance of *BLM*$^{-/-}$ cells to γ-irradiation is reminiscent of the observation that cells exposed to low-dose ionizing radiation or hydrogen peroxide are less sensitive to high-dose ionizing radiation [27]. Our previous studies suggest that slightly more DNA lesions occur when there is a defect in BLM. Thus it seems likely that the slight resistance of *BLM*$^{-/-}$ cells to γ-irradiation is caused by the activation of the DSB repair system due to an increase in DSBs in *BLM*$^{-/-}$ cells under conditions not inducing damage.

Methyl methanesulfonate (MMS) causes the methylation of DNA bases, and a methylated base such as 3-methyladenine is thought to block DNA replication [28]. Recent studies using prokaryotic and eukaryotic cells indicated that the Holliday junctions are formed at arrested replication forks [16,29], and the cleavage of such junctions leads to the formation of DSBs at arrested replication forks [16]. We previously suggested that the physiological function of BLM is to resolve Holliday junctions. If this is the case, the number of DSBs will be considerably increased upon exposure to MMS in BLM-defective cells. However, the sensitivity of *ATM*$^{-/-}$/*BLM*$^{-/-}$ DT40 cells to MMS was similar to that of *BLM*$^{-/-}$ DT40 cells, indicating that ATM is not essential to the repair of DSBs formed in *BLM*$^{-/-}$ cells on exposure to MMS.

The defect of ATM only slightly reduced the increased SCE in *BLM*$^{-/-}$ DT40 cells, indicating a minor contribution of ATM to the formation of SCE in *BLM*$^{-/-}$ DT40 cells. We previously suggested that the defect of BLM causes the formation of DSBs during DNA replication, and these DSBs are repaired mainly by homologous recombination, resulting in an increased incidence of SCE [20]. Thus, the small contribution of ATM to the formation of SCE in *BLM*$^{-/-}$ DT40 is not surprising because DNA lesions formed during DNA replication could be recognized by ATR instead of ATM.

It has been reported that p53 binds to BLM in vivo and in vitro and localizes at stalled DNA replication sites depending on BLM [30]. In addition, the depletion of p53 in the cells derived from a Bloom syndrome individual slightly increased the frequency of SCE. Thus, it is interesting to analyze the functional relationship between BLM and p53. However, DT40 cells do not express p53 [21], and the phenotypes of *ATM*$^{-/-}$, *BLM*$^{-/-}$, and *ATM*$^{-/-}$/*BLM*$^{-/-}$ DT40 cells represent those of these cells in the absence of p53. It seems likely that the increase in the frequency of SCE in *BLM*$^{-/-}$ and *ATM*$^{-/-}$/*BLM*$^{-/-}$ DT40 cells involves the contribution of the defects in both BLM and p53 although the contribution of p53 is small.

It has been reported that a defect of ATM causes the slower accumulation of RAD51 foci in response to ionizing radiation [31], and ATM phosphorylates BRCA1, NBS1 and Rad51 [32–35]. In addition, a defect in BRCA1 reduces homologous recombination [36]. These results indicate that ATM is somehow involved in homologous recombination. The defect of ATM partially reduced the increased targeted integration frequency in *BLM*$^{-/-}$ DT40 cells, indicating the involvement of ATM in homologous recombination. It seems likely that in the case of targeted integration, there exist double strand DNA ends of transfected DNA regardless of DNA replication and these double strand DNA ends are recognized by ATM.

In summary, although BLM is phosphorylated by ATM in response to ionizing radiation [15], and BLM and ATM are components of BASC [14], we could find little functional relationship between BLM and ATM. While circumstantial evidence strongly indicates the formation of DSBs in *BLM*$^{-/-}$ DT40 cells under MMS-exposed and non-exposed conditions, the contribution of ATM to the repair of DSBs formed in *BLM*$^{-/-}$ DT40 cells, seems to be very small. We speculate that the DSBs that are formed during DNA replication in the absence of BLM are specifically channeled to a homologous recombination pathway via components of BASC other than ATM, such as BRCA1 and RAD50/MRE11/NBS1. The identification of such channeling factors among the components of BASC will shed light on the function of BASC.

Acknowledgements

We thank Dr. Takeda for kindly providing the *RAD54*-Hygromycin® vector. This work was supported by Grants-in-Aid for Scientific Research from the Ministry of Education, Culture, Science, Sports, and Technology of Japan, a Health Sciences Research Grant from the Ministry of Health, Labor, and Welfare of Japan, and a grant from the Uehara Memorial Foundation. M. Seki was supported in part by the Mochida Memorial Foundation for Medical and Pharmaceutical Research.

References

[1] J. German, Bloom syndrome: a mendelian prototype of somatic mutational disease, Medicine (Baltimore) 72 (1993) 393–406.
[2] R. Hand, J. German, A retarded rate of DNA chain growth in Bloom's syndrome, Proc. Natl. Acad. Sci. U. S. A. 72 (1975) 758–762.
[3] U. Lonn, S. Lonn, U. Nylen, G. Winblad, J. German, An abnormal profile of DNA replication intermediates in Bloom's syndrome, Cancer Res. 50 (1990) 3141–3145.
[4] S. Liao, J. Graham, H. Yan, The function of *Xenopus* Bloom's syndrome protein homolog (xBLM) in DNA replication, Genes Dev. 14 (2000) 2570–2575.
[5] M.C. Paterson, P.J. Smith, Ataxia telangiectasia: an inherited human disorder involving hypersensitivity to ionizing radiation and related DNA-damaging chemicals, Annu. Rev. Genet. 13 (1979) 291–318.
[6] K. Savitsky, A. Bar-Shira, S. Gilad, G. Rotman, Y. Ziv, L. Vanagaite, D.A. Tagle, S. Smith, T. Uziel, S. Sfez, A single ataxia telangiectasia gene with a product similar to PI-3 kinase, Science 268 (1995) 1749–1753.
[7] C.E. Canman, D.S. Lim, K.A. Cimprich, Y. Taya, K. Tamai, K. Sakaguchi, E. Appella, M.B. Kastan, J.D. Siliciano, Activation of the ATM kinase by ionizing radiation and phosphorylation of p53, Science 281 (1998) 1677–1679.
[8] S. Banin, L. Moyal, S. Shieh, Y. Taya, C.W. Anderson, L. Chessa, N.I. Smorodinsky, C. Prives, Y. Reiss, Y. Shiloh, Y. Ziv, Enhanced phosphorylation of p53 by ATM in response to DNA damage, Science 281 (1998) 1674–1677.
[9] R. Baskaran, L.D. Wood, L.L. Whitaker, C.E. Canman, S.E. Morgan, Y. Xu, C. Barlow, D. Baltimore, A. Wynshaw-Boris, M.B. Kastan, J.Y. Wang, Ataxia telangiectasia mutant protein activates c-Abl tyrosine kinase in response to ionizing radiation, Nature 387 (1997) 516–519.
[10] T. Shafman, K.K. Khanna, P. Kedar, K. Spring, S. Kozlov, T. Yen, K. Hobson, M. Gatei, N. Zhang, D. Watters, M. Egerton, Y. Shiloh, S. Kharbanda, D. Kufe, M.F. Lavin, Interaction between ATM protein and c-Abl in response to DNA damage, Nature 387 (1997) 520–523.
[11] S. Matsuoka, M. Huang, S.J. Elledge, Linkage of ATM to cell cycle regulation by the Chk2 protein kinase, Science 282 (1998) 1893–1897.
[12] K. Tominaga, H. Morisaki, Y. Kaneko, A. Fujimoto, T. Tanaka, M. Ohtsubo, M. Hirai, H. Okayama, K. Ikeda, M. Nakanishi, Role of human Cds1 (Chk2) kinase in DNA damage checkpoint and its regulation by p53, J. Biol. Chem. 274 (1999) 31463–31467.
[13] N.H. Chehab, A. Malikzay, M. Appel, T.D. Halazonetis, Chk2/hCds1 functions as a DNA damage checkpoint in G(1) by stabilizing p53, Genes Dev. 14 (2000) 278–288.
[14] Y. Wang, D. Cortez, P. Yazdi, N. Neff, S.J. Elledge, J. Qin, BASC, a super complex of BRCA1-associated proteins involved in the recognition and repair of aberrant DNA structures, Genes Dev. 14 (2000) 927–939.
[15] M. Ababou, S. Dutertre, Y. Lecluse, R. Onclercq, B. Chatton, M. Amor-Gueret, ATM-dependent phosphorylation and accumulation of endogenous BLM protein in response to ionizing radiation, Oncogene 19 (2000) 5955–5963.
[16] M. Seigneur, V. Bidnenko, S.D. Ehrlich, B. Michel, RuvAB acts at arrested replication forks, Cell 95 (1998) 419–430.
[17] N.A. Ellis, J. Groden, T.Z. Ye, J. Straughen, D.J. Lennon, S. Ciocci, M. Proytcheva, J. German, The Bloom's syndrome gene product is homologous to RecQ helicases, Cell 83 (1995) 655–666.
[18] J.K. Karow, R.K. Chakraverty, I.D. Hickson, The Bloom's syndrome gene product is a 3′–5′ DNA helicase, J. Biol. Chem. 272 (1997) 30611–30614.
[19] J.K. Karow, A. Constantinou, J.L. Li, S.C. West, I.D. Hickson, The Bloom's syndrome gene product promotes branch migration of Holliday junctions, Proc. Natl. Acad. Sci. U. S. A. 97 (2000) 6504–6508.
[20] W. Wang, M. Seki, Y. Narita, E. Sonoda, S. Takeda, K. Yamada, T. Masuko, T. Katada, T. Enomoto, Possible association of BLM in decreasing DNA double strand breaks during DNA replication, EMBO J. 19 (2000) 3428–3435.
[21] N. Takao, H. Kato, R. Mori, C. Morrison, E. Sonada, X. Sun, H. Shimizu, K. Yoshioka, S. Takeda, K. Yamamoto, Disruption of ATM in p53-null cells causes multiple functional abnormalities in cellular response to ionizing radiation, Oncogene 18 (1999) 7002–7009.
[22] E. Sonoda, M.S. Sasaki, C. Morrison, Y. Yamaguchi-Iwai, M. Takata, S. Takeda, Sister chromatid exchanges are mediated by homologous recombination in vertebrate cells, Mol. Cell. Biol. 19 (1999) 5166–5169.
[23] K. Suzuki, S. Kodama, M. Watanabe, Recruitment of ATM protein to double strand DNA irradiated with ionizing radiation, J. Biol. Chem. 274 (1999) 25571–25575.
[24] K.K. Khanna, S.P. Jackson, DNA double-strand breaks: signaling, repair and the cancer connection, Nat. Genet. 27 (2001) 247–254.
[25] O. Bischof, S.H. Kim, J. Irving, S. Beresten, N.A. Ellis, J. Campisi, Regulation and localization of the Bloom syndrome protein in response to DNA damage, J. Cell Biol. 153 (2001) 367–380.
[26] L. Wu, S.L. Davies, N.C. Levitt, I.D. Hickson, Potential role for the BLM helicase in recombinational repair via a conserved interaction with RAD51, J. Biol. Chem. 276 (2001) 19375–19381.
[27] I. Szumiel, Monitoring and signaling of radiation-induced damage in mammalian cells, Radiat. Res. 150 (1998) S92–S101.
[28] M. Kupiec, Damage-induced recombination in the yeast *Saccharomyces cerevisiae*, Mutat. Res. 451 (2000) 91–105.
[29] H. Zou, R. Rothstein, Holliday junctions accumulate in replication mutants via a RecA homolog-independent mechanism, Cell 90 (1997) 87–96.
[30] S. Sengupta, S.P. Linke, R. Pedeux, Q. Yang, J. Farnsworth, S.H. Garfield, K. Valerie, J.W. Shay, N.A. Ellis, B. Wasylyk, C.C. Harris,

BLM helicase-dependent transport of p53 to sites of stalled DNA replication forks modulates homologous recombination, EMBO J. 22 (2003) 1210–1222.
[31] C. Morrison, E. Sonoda, N. Takao, A. Shinohara, K. Yamamoto, S. Takeda, The controlling role of ATM in homologous recombinational repair of DNA damage, EMBO J. 19 (2000) 463–471.
[32] D. Cortez, Y. Wang, J. Qin, S.J. Elledge, Requirement of ATM-dependent phosphorylation of brca1 in the DNA damage response to double-strand breaks, Science 286 (1999) 1162–1166.
[33] D.S. Lim, S.T. Kim, B. Xu, R.S. Maser, J. Lin, J.H. Petrini, M.B. Kastan, ATM phosphorylates p95/nbs1 in an S-phase checkpoint pathway, Nature 404 (2000) 613–617.
[34] S. Zhao, Y.C. Weng, S.S. Yuan, Y.T. Lin, H.C. Hsu, S.C. Lin, E. Gerbino, M.H. Song, M.Z. Zdzienicka, R.A. Gatti, J.W. Shay, Y. Ziv, Y. Shiloh, E.Y. Lee, Functional link between ataxia-telangiectasia and Nijmegen breakage syndrome gene products, Nature 405 (2000) 473–477.
[35] G. Chen, S.S. Yuan, W. Liu, Y. Xu, K. Trujillo, B. Song, F. Cong, S.P. Goff, Y. Wu, R. Arlinghaus, D. Baltimore, P.J. Gasser, M.S. Park, P. Sung, E.Y. Lee, Radiation-induced assembly of Rad51 and Rad52 recombination complex requires ATM and c-Abl, J. Biol. Chem. 274 (1999) 12748–12752.
[36] M.E. Moynahan, J.W. Chiu, B.H. Koller, M. Jasin, Brca1 controls homology-directed DNA repair, Mol. Cell 4 (1999) 511–518.

Available online at www.sciencedirect.com
SCIENCE DIRECT®
ELSEVIER
Mutation Research 560 (2004) 133–145
MR
Genetic Toxicology and Environmental Mutagenesis
www.elsevier.com/locate/gentox
Community address: www.elsevier.com/locate/mutres

Further characterization of loss of heterozygosity enhanced by p53 abrogation in human lymphoblastoid TK6 cells: disappearance of endpoint hotspots

Fumio Yatagai[a,*], Shigeko Morimoto[a], Takesi Kato[a], Masamitsu Honma[b]

[a] *Division of Radioisotope Technology, The Institute of Physical and Chemical Research (RIKEN), Saitama 351-0198, Japan*
[b] *Division of Genetics and Mutagenesis, National Institute of Health Science, Tokyo 158-8501, Japan*

Received 7 August 2003; received in revised form 19 February 2004; accepted 19 February 2004

Abstract

Loss of heterozygosity (LOH) is the predominant mechanism of spontaneous mutagenesis at the heterozygous thymindine kinase locus (*tk*) in TK6 cells. LOH events detected in spontaneous TK^- mutants (110 clones from p53 wild-type cells TK6-20C and 117 clones from p53-abrogated cells TK6-E6) were analyzed using 13 microsatellite markers spanning the whole of chromosome 17. Our analysis indicated an approximately 60-fold higher frequency of terminal deletions in p53-abrogated cells TK6-E6 compared to p53 wild-type cells TK6-20C whereas frequencies of point mutations (non-LOH events), interstitial deletions, and crossing over events were found to increase only less than twofold by such p53 abrogation. We then made use of an additional 17 microsatellite markers which provided an average map-interval of 1.6 Mb to map various LOH endpoints on the 45 Mb portion of chromosome 17q corresponding to the maximum length of LOH tracts (i.e. from the distal marker D17S932 to the terminal end). There appeared to be four prominent peaks (I–IV) in the distribution of LOH endpoints/Mb of Tk6-20C cells that were not evident in p53-abrogated cells TK6-E6, where they appeared to be rather broadly distributed along the 15–20 Mb length (D17S1807 to D17S1607) surrounding two of the peaks that we detected in TK6-20C cells (peaks II and III). We suggest that the chromosomal instability that is so evident in TK6-E6 cells may be due to DNA double-strand break repair occurring through non homologous end-joining rather than allelic recombination.

Keywords: Loss of heterozygosity (LOH); p53 Abrogation; Thymidine kinase locus (*tk*); Human lymphoblastoid cell

1. Introduction

Multistage carcinogenesis is often associated with the accumulation of chromosomal rearrangements, such as translocations, terminal deletions, interstitial deletions or amplifications [1,2]. Such chromosomal alterations can engender loss of heterozygosity (LOH), leading to the inactivation of tumor-suppressor genes that is characteristic of a great many cancer cells [3,4]. Elucidation of the mechanisms that lead to LOH is therefore important in understanding the origins and progression of cancer, given that these processes are not well understood as yet. This may be due to the complexity and large size of mammalian genomes, making it difficult to determine the precise chromosomal breakpoints associated with LOH events [5,6]. Recently there have been a number of systematic

Abbreviations: DSBs, double-strand breaks; NHEJ, non homologous end-joining; HR, homologous recombination

* Corresponding author. Tel.: +81-48-467-9566; fax: +81-48-462-4636.
E-mail address: yatagai@postman.riken.go.jp (F. Yatagai).

1383-5718/$ – see front matter © 2004 Elsevier B.V. All rights reserved.
doi:10.1016/j.mrgentox.2004.02.012

studies of spontaneous- and mutagen-induced LOH events and genome instability in *Saccharomyces cerevisiae* which relied upon well-characterized genetic techniques and were facilitated by accessibility to the complete yeast genome database [7–10]; these studies suggest the existence of a number of pathways that cooperate to suppress genome instability. Double-strand breaks (DSBs) in DNA can be processed by various mechanisms that result in different outcomes, including: (i) homologous recombination (HR), i.e., either nonallelic recombination resulting in sister chromatid exchanges (SCE) or allelic recombination causing homozygous LOH; (ii) nonhomologous end-joining (NHEJ) resulting in translocations or deletions (hemizygous LOH); (iii) single-strand annealing (SSA) between direct repeats yielding small deletions; (iv) break-induced replication (BIR) producing translocations (hemizygous LOH) or large tracts of gene conversions (homozygous LOH); (v) telomere addition causing terminal deletions (hemizygous LOH); or (vi) complete chromosome loss. While caution is certainly called for when extrapolating results from yeast to humans, detailed molecular features of LOH events in yeast may be a useful starting-point, especially when systematic LOH studies in higher eukaryotes are lacking.

There have been numerous LOH mapping studies in human cancer cells, but most of these have focused on a restricted number of specific tumor-suppressor genes. Several human cell lines that carry a recessive heterozygous mutation at an autosomal locus have been established for the studies of mutagenesis [11–13]. For example, the human lymphoblastoid cell line TK6 has been used frequently in LOH studies because it carries dipolymorphic one-base insertion frameshift mutations in the thymidine kinese (*tk*) locus (i.e., an inactivating +1 frameshift mutation in exon 4 of the nonfunctional allele, and a silent frameshift in exon 7 of the functional allele). These mutations facilitate the detection of LOH events as well as sequence analysis of intragenic mutations at the *tk* locus [14,15]. Using this cell line, it has been shown that a high proportion (60–70%) of spontaneous TK^- mutants exhibit LOH [16,17], and that LOH tracts in many of these mutants extend towards the terminal end of chromosome 17q [18]. These features of spontaneous LOH events are not specific to TK6 cells, but instead are fairly common in mammalian cells. As reported in a study of human cells heterozygous at the *aprt* locus, LOHs are the predominant spontaneous mutational events and many of those LOH tracts are very long [5,13]. We have previously described an improved version of the TK6 system which allows LOHs along the whole length of chromosome 17 to be detected more efficiently [19]. Our analysis of LOH events in both p53-wild type and p53-abrogated derivatives of TK6 led us to consider that spontaneous DSBs appear to be promptly repaired through recombination between homologous chromosomes in p53 wild-type cells, thereby implying (as much other data does) that the p53 protein contributes to the maintenance of genome integrity.

Our present study was concerned with further characterizing LOH events in cells in which p53 has been abrogated, and involved the analysis of large numbers of spontaneous LOH events at the *tk* locus in the TK6 system. We also mapped the LOH endpoints of those mutants along chromosome 17q at average intervals of 1.6 Mb. The results of these analyses suggest that the genomic instability that we see in the p53-abrogeted cells is much more likely to result from DSB repair through non homologous endjoining (NHEJ) than from allelic recombination.

2. Materials and methods

2.1. Cell lines

The TK6 human lymphoblastoid cell line is functionally heterozygous at the *tk* locus [14]. TK6-E6-5E (referred to as TK6-E6 throughout this manuscript) and TK6-20C are, respectively, a functionally-p53-deficient TK6 derivative which expresses the HPV16 E6 protein from a CMV-driven plasmid vector, and a p53-wild type TK6 derivative carrying an empty vector [20]. Cells were grown at 37 °C 5% CO_2 in RPMI 1640 medium (Gibco–BRL, Grand Island, NY) supplemented with 200 μg/ml sodium pyruvate and 10% heat inactivated horse serum (JRH Biosciences, Lenexa, KS).

2.2. TK^- mutant collection

Protocols for selection of spontaneous TK^- mutants have been described previously [19]. Briefly, in-

dependent cultures were treated with CHAT medium (RPMI medium supplemented with 10 μM deoxycytidine, 200 μM hypoxanthine, 0.2 μM aminopterin and 17.5 μM thymidine) to eliminate pre-existing TK^- mutants. The cells were grown in fresh RPMI medium for a few days until the cell density reached $\sim 1 \times 10^6$ cells/ml. TK-deficient mutant clones were then isolated by seeding cells from each independent culture into 96-well microwell plates at 2×10^4 cells per well, in RPMI medium containing 4 μg/ml trifluorothymidine (TFT). The plates were incubated at 37 °C in a 5% CO_2 incubator for 10 days to select the TK^- mutants (early mutants) and the incubation was extended until total 24 days for the selection of mutants (late mutants). Frequencies of spontaneous TK^- mutants were calculated based on a Poisson distribution.

2.3. LOH analysis by polymerase chain reaction (PCR)

TK6-20C carries dipolymorphic, single-base insertion frameshifts within the coding sequence of *tk*. The non-functional allele expresses an inactivating frameshift occurring in a run of cytosine residues in exon 4, while the functional counterpart carries a phenotypically silent frameshift within a run of guanine residues in exon 7 [14]. We previously described a method for the co-amplification of the dipolymorphic sites of exon 4 and 7, together with a part of the β-globin gene on chromosome 11 as a control marker [19]. Two additional microsatellite markers D17S937 and D17S802 flanking the *tk* locus, were also used to define the extent of LOH tracts. The PCR products were analyzed with an ABI310 genetic analyzer, and processed with Gene Scan software (PE Biosystems, Chiba, Japan) to determine LOH status at the *tk* locus.

2.4. Gross analysis of LOH tracts on chromosome 17

TK^- mutants determined to be either homozygous or hemizygous at the *tk* locus were then subjected to multiplex PCR with 10 microsatellite makers, D17S1566, THRA1, D17S1299, D17S932, D16S588, D17S807, D17S789, D17S785, D17S784 and D17S928 (Table 1), roughly distributed over the whole of chromosome 17. The multiplex PCR products were labeled with fluorescent dyes and applied to the ABI310 analyzer on a capillary gel. It was difficult to quantify the copy numbers of each PCR product directly from the profile because of the lack

Table 1
Polymorphic microsatellite markers used for the analysis of LOH events on chromosome 17

Microsatellite markers[a]	Position on chrmosome 17 (bp)[b]
115B1 (D17S1566)	2575569–2575757
THRA	42199292–42264954
CHLC (D17S1299)	43005530–43005724
AFM248yg9 (D17S932)	44769576–44769876
AFM240yg7 (D17S930)	47244603–47246153
AFM248yg1 (D17S810)	48011861–48012187
AFM298wa5 (D17S950)	48405672–48406022
AFM234td2 (D17S806)	51396410–51396636
AFMb010xa5 (D17S1827)	52260730–52261019
AFM301ye5 (D17S1868)	52986746–52987087
42D6 (D17S588)	53884277–53884521
AFM248tb9 (D17S809)	55714379–55714721
AFM095zd11 (D17S788)	56118569–56118810
AFMc023xc5 (D17S1865)	56513136–56513504
AFM095tc5 (D17S787)	59245440–59245796
AFMa046zg1 (D17S1607)	59776938–59777312
AFM338xg5 (D17S1606)	61647986–61648349
CHLC.GATA49C09 (D17S1290)	62376359–62376692
AFM200va9 (D17S923)	64646272–64646588
AFM168xd12 (D17S794)	67176348–67176669
AFM291ve9 (D17S948)	67646368–67646657
ATA8B07 (D17S1297)	68669230–68669520
AFM269yf1 (D17S942)	70677622–70677998
AFM234xc9 (D17S807)	70957194–70957541
AFMa300xa5 (D17S1813)	71555861–71556176
AFM107yb8 (D17S789)	72986844–72987157
AFM268yd5 (D17S940)	74521227–74521623
AFM207vf4 (D17S840)	75054282–75054649
AFMa202xd1 (D17S1797)	76971341–76971663
AFMa247zg9 (D17S1352)	78975856–78976249
AFMa247xc5 (D17S1807)	79209191–79209577
AFMa135xd5 (D17S1603)	81300774–81301112
AFM049xc1 (D17S785)	81667709–81667990
AFM107ye3 (D17S937)	82596930–82597254
tk	
AFM210xa5 (D17S802)	83546042–83546313
AFM044xg3 (D17S784)	85620230–85620529
AFM217yd10 (D17S928)	88330559–88330860

[a] Information about polymorphic microsatellite makers and PCR primer sequences were obtained from "human genome resources" in NCBI (http://www.ncbi.nih.gov). Microsatellite markers shown by bold letter were those used in our previous study [19].

[b] Sequence positions of microsatellite markers were obtained from UCSC Genome Browser Gateway (http://genome.ucsc.edu/cgi-bin/hgGateway?db=hg10).

of a reliable control PCR marker. We therefore extrapolated the defined zygosity of LOH (i.e., homozygous or hemizygous) at the *tk* locus to the LOH status as determined at the 10 marker sites.

2.5. Mapping of LOH endpoints on the defined portion of chromosome 17q

Since the multiplex PCR results showed that no LOH event extended over the distal marker D17S932 in either cell line, mapping of LOH endpoints was restricted on the 45 Mb long 17q arm, and so extended from D17S932 to the telomere. Microsatellite makers used for the mapping were first surveyed in the NCBI Human Genome Database (http://www.ncbi.nih.go) and then tested with TK6-20C cells for their effectiveness. PCR primers and their positions on chromosome 17q are presented in Table 1, including those used in the 10 mix multiplex PCR (protocols of the all PCR experiments described in this report are available on request). Forward primers were labeled with one of three fluorescent dyes (all primers were purchased from GENSET, Kyoto, Japan). Based on the results of gross analysis of LOH tracts, TK^- mutants were assigned into five groups; group 1 cells exhibited LOH endpoints between D17S932 and D17S588 (fragment 1, 9.11 Mb), group 2 between D17S588 and D17S807 (fragment 2, 17.1 Mb), group 3 between D17S807 and D17S789 (fragment 3, 2.03 Mb), group 4 between D17S789 and D17S785 (fragment 4, 8.68 Mb) and group 5 between D17S785 and D17S928 (fragment 5, 6.66 Mb). Microsatellite markers used for the mapping were: 6 markers for fragment 1, 12 for fragment 2, 1 for fragment 3, and 6 for fragment 4. Fragment 2 was very large and so many mutants were assigned to it; it was therefore further divided into four segments by multiplex PCR with the 4 primers D17S788, D17S1607, D17S1606 and D17S794, followed by PCR with the primers listed in Table 1 for each segment.

3. Results

3.1. Mutation frequency and LOH analysis of TK^- mutants

The frequency of spontaneous TK^- mutants was 5.7-fold higher in TK6-E6 cells than in TK6-20C cells (Table 2), a figure which is not too different from our previous estimate of 8.8-fold [19]. For a detailed characterization of LOH events associated with the abrogation of p53, we isolated larger numbers of spontaneous TK^- mutants from the two cell-lines, and analyzed 110 mutants derived from TK6-20C and 117 mutants derived from TK6-E6 for judgement of LOH at the dipolymorphic sites in exons 4 and 7 of the *tk* locus (Table 2). LOH was not detected in 43 of the 110 (39.0%) mutants of TK6-20C or in 8 of the 117 (6.8%) mutants of TK6-E6. Direct sequencing

Table 2
Spontaneous mutation frequencies and LOH status of TK^- mutants

Cell line	p53 status[a]	TK^- mutation frequency[b] ($\times 10^{-6}$)	Number of TK^- mutants analyzed[c]		LOH status of TK^- mutations			
					Non-LOH	Hemizygous	Homozygous	Others[d]
TK6-20C	Wild type	5.7 ± 1.3	Early	34	31	3	0	0
			Late	76	12	7	56	1
				110	43 (39.0%)	10 (9.1%)	56 (51.0%)	1 (0.9%)
TK6-E6	Deficient	32.7 ± 3.2	Early	5	5	0	0	0
			Late	112	3	85	20	4
				117	8 (6.8%)	85 (72.6%)	20 (17.1%)	4 (3.5%)

[a] p53 in TK6-E6 cells is degraded by the HPV16 E6 gene product and can not be detected by western blot analysis of the cell extract [19].
[b] Average of three separate experiments.
[c] Early and late TK^- mutants were, respectively, isolated at 10 days and 24 days of selection in TFT medium.
[d] Estimated copy numbers of exon 4 or exon 7 in these mutants (20C L-10, E6 L-2, L-15, L-103 and L-110) were too large or small than the expected number 1 or 2.

of cDNAs showed that the mutations that had occurred in these non-LOH mutants were point mutations, i.e., were base substitutions, frameshifts or deletions of a few bases (data not shown). The lower rate of point mutations, 6.8% in TK6-E6 compared to 39% in TK6-20C, could be considered as the result of 5.7-fold enhancement of TK^- mutation frequency. In other words, the real occurrence of point mutations was not changed by the p53 status. More frequent recovery of point mutations in early mutants compared to those in late mutants was common to both cell lines, reflecting that point mutation was fixed in the early stage of cell proliferation in the selection medium.

A few of the TK^- mutants were not proved to have resulted from either homozygous or hemizygous LOH events. In this case, the relative ratio of the peak area of either the exon 4 or exon 7 PCR product, normalized to the coamplified part of β-globin, deviated extensively from the standard ratio of 1 (hemizygous) or 2 (homozygous), suggesting that as yet unidentified chromosomal alterations may have occurred. A substantially majority of the mutants in the TK6-E6 background (85/117 or 73%) were the result of hemizygous LOH events, whereas nearly half of the mutants in Tk6-20C cells (56/110 or 51%) were the result of homozygous LOH events. Extensive LOHs spanning the flanking markers D17S937 and D17S802 were observed in 67/110 of the TK6-20C mutants and in 109/117 of the TK6-E6 mutants. Similar propotions of LOH events among TK^- mutants were noted in our previous work [19].

3.2. Analysis of LOH tracts on chromosome 17

A set of 10 polymorphic microsatellite markers was used to determine the lengths of the various LOH tracts

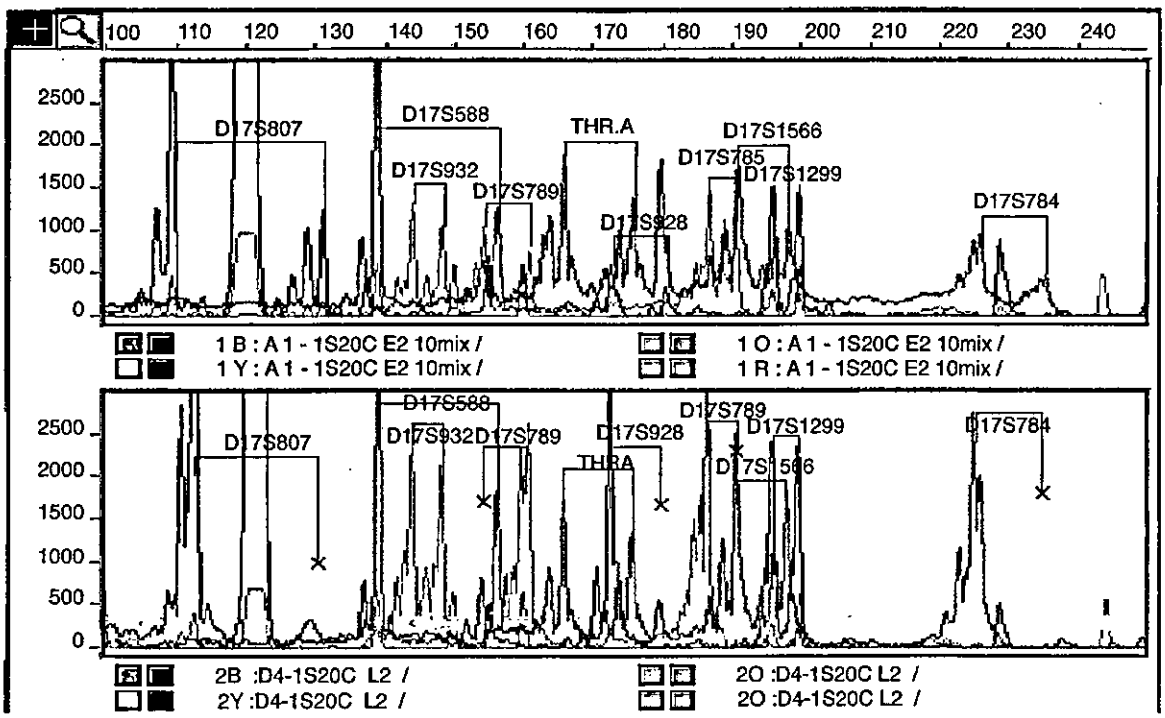

Fig. 1. Representative profiles of multiplex PCR with TK^- mutants. PCR primers of 10 polymorphic microsatellite markers were labeled with either one of the three fluorescent dyes, green, blue or black. The size markers are labeled red. The profile shown at upper panel is an example of non-LOH mutants and that at lower panel is from a LOH mutant. Each pair of PCR products are indicated by line and deleted PCR products are indicated by cross.

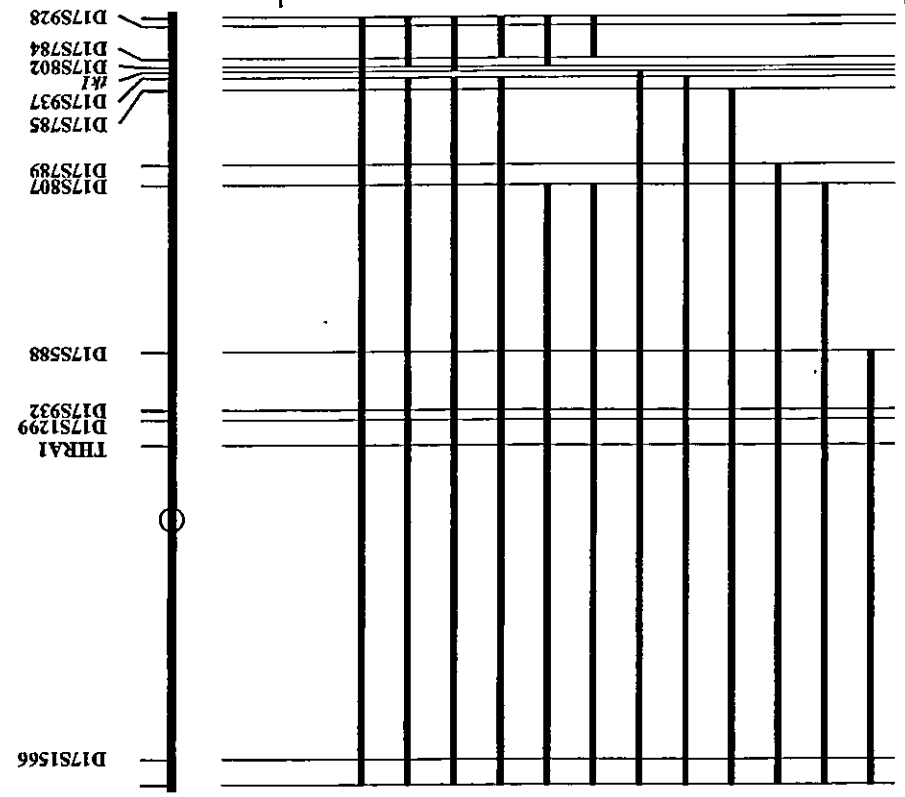

Mutational event	TK6-E6 Early	TK6-E6 Late	TK6-E6 Total	TK6-20C Early	TK6-20C Late	TK6-20C Total
Point mutation	5	3	8 (6.8%)	31	12	43 (39.1%)
Tk1 dele.	0	0	0 (0.0%)	3	4	7 (6.4%)
D17S937-ex.7	0	0	0 (0.0%)	0	1	1 (0.9%)
D17S937-D17S784	0	1	1 (0.9%)	0	1	1 (0.9%)
D17S807-D17S802	0	0	0 (0.0%)	0	1	1 (0.9%)
D17S807-D17S784	0	0	0 (0.0%)	0	1	1 (0.9%)
ex.4-D17S928	0	2	2 (1.7%)	0	1	1 (0.9%)
D17S937-D17S928	0	5	5 (4.3%)	0	5	5 (4.5%)
D17S785-D17S928	0	28	28(23.9%)	0	14	14 (12.7%)
D17S789-D17S928	0	16	16 (13.7%)	0	4	4 (3.6%)
D17S887-D17S928	0	55	55 (47.0%)	0	16	16 (14.6%)
D17S588-D17S928	0	2	2 (1.7%)	0	16	16 (14.6%)
Total	5	112	117	34	76	110

Fig. 2. Lengths of LOH tracts in spontaneous TK$^-$ mutants from TK6-20C and TK6-E6. Relative sequence positions of 10 microsatellite markers on chromosome 17 are shown at the upper part. Multiplex PCR with 10 primers was performed with 110 and 117 spontaneous TK$^-$ mutants, respectively, from TK6-20C and TK6-E6. LOH tracts indicated by blank space are the minimum length, as the real endpoint of LOH tracts would be between the terminal position of LOH tracts shown and the next marker's position.